ChemComm

COMMUNICATION

View Article Online
View Journal | View Issue

Cite this: *Chem. Commun.*, 2018, **54**, 7362

Received 22nd May 2018,
Accepted 7th June 2018

DOI: 10.1039/c8cc04080j

rsc.li/chemcomm

Macrocycle crosslinked mesoporous polymers for ultrafast separation of organic dyes†

Qian Zhao[a] and Yu Liu *[ab]

Mesoporous polymers were synthesized by interfacial polymerization of macrocycles (sulfonatocalix[4]arenes and pillar[5]arenes) and terephthaloyl chloride. These polymer films showed ultrahigh permeabilities and excellent selectivities for molecular separations of organic dyes in water.

Effluents from textile and dyestuff industries often contain organic dyes which could induce mutations to living organisms, so separation and removal of dyes from wastewater is urgently required for environmental protection and human health.[1] Owing to the low energy consumption, the membrane-separation process becomes a very important technology for water treatment and selective molecular separations.[2] Considering most dye molecules are larger than 0.5 nm and smaller than 2 nm, lots of microporous membranes (with the pore size <2 nm) have been developed, such as metal–organic framework films,[3] covalent–organic framework films,[4] zeolite films,[5] graphene-based films,[6] microporous polymers and polymers of intrinsic microporosity films.[7] These films showed certain solvent permeances and good selectivities for molecular separations. However, the mass transport rates are usually relatively low due to the strong confinement in the microporous materials (Fig. 1a).[8] Besides increasing the areas and decreasing the thicknesses of the microporous membranes, developing new membrane materials with high transport properties and good selectivities for dye separations remains a challenge both for academic and industrial scientists.[9]

It is well known that the mesoporous materials with relatively large pore sizes (2–50 nm) have better mass diffusion and transfer properties but lack selectivities for small molecules.[10] Incorporating extra binding sites to mesoporous materials is a feasible method for fabricating a new kind of adsorptive polymer material (Fig. 1b).[11] Therefore, macrocycles especially cyclodextrin[12] and calixarene,[13] of which the complexation with dyes has been extensively and systematically studied,[14] have been employed as effective candidate materials for the removal of organic pollutants from wastewater. Meanwhile, interfacial polymerizations have been established for the construction of microporous ultrathin films with a thickness of a few tens of nanometers recently.[4,7a,12a,b,15] It seems reasonable to develop mesoporous polymers of crosslinked macrocycles *via* interfacial polymerization. Herein, we utilized terephthaloyl chloride (TC) to crosslink three macrocyclic molecules (calix[4]arene (C4A), pillar[5]arene (P5A) and sulfonatocalix[4]arene (SC4A)[16]) on the surface of commercial polyethersulfone (PES) or Nylon6 porous membranes respectively (Fig. 2 and 1b). Fortunately, the obtained polymers with mesopores gave good molecular separations for organic dyes in water and showed ultrahigh permeances for both polar and nonpolar solvents.

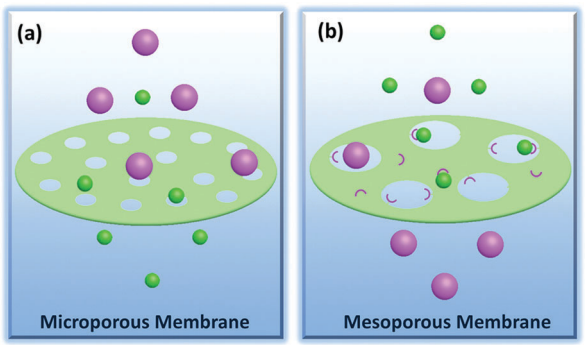

Fig. 1 (a) Microporous membrane with size selectivity and lower permeability (conventional strategy for membrane separation); (b) mesoporous membrane with higher permeability and selective adsorption of small molecules *via* host–guest complexation (our strategy).

A key factor in the fabrication of these films was the pH value of the aqueous phase. As shown in Table S1 (ESI†), when the mass fraction of SC4A was fixed at 5% and the mass fraction of NaOH was below 0.5%, films with tiny holes were formed, which could be attributed to insufficient crosslinking under the

[a] *College of Chemistry, State Key Laboratory of Elemento-Organic Chemistry, Nankai University, Tianjin 300071, P. R. China*
[b] *Collaborative Innovation Center of Chemical Science and Engineering (Tianjin), Nankai University, Tianjin 300072, P. R. China. E-mail: yuliu@nankai.edu.cn*

† Electronic supplementary information (ESI) available. See DOI: 10.1039/c8cc04080j

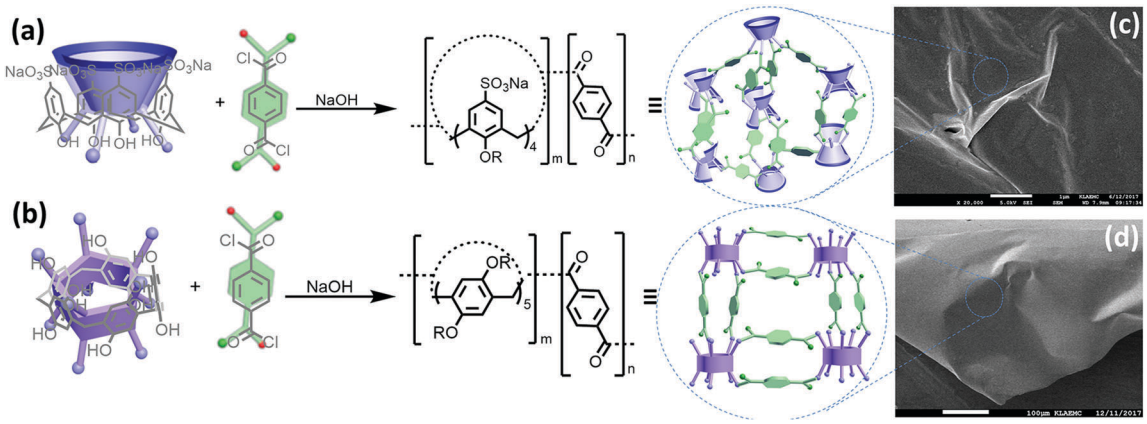

Fig. 2 pTC-SC4A films and pTC-P5A films made *via* interfacial polymerization. (a and b) Synthetic routes of films from SC4A or P5A (dissolved in NaOH solution) and TC (dissolved in organic phase) respectively; (c and d) SEM images of pTC-SC4A (synthesized from 5% SC4A and 1% NaOH aqueous solution and 0.5% TC in *n*-hexane at room temperature) or pTC-P5A films (2% P5A in 1.6% NaOH aqueous solution, 0.5% TC in *n*-hexane at room temperature).

weak alkaline conditions (Fig. S4a–c, ESI†). However, when the mass fraction of NaOH was increased to 1% ([hydroxyl of SC4A] : [NaOH] = 1 : 1.2), transparent and flexible films with no defects could be formed easily (Fig. S4d–f, ESI†), indicating the effective esterification. As shown in Fig. 3a, the pure and entire pTC-SC4A film floated in DMF was robust but flexible, which showed no visible damage after suction with a plastic pipet (Video S1, ESI,† for pTC-SC4A film). When the mass fraction of NaOH was increased to 2%, films with lots of dots on the surface formed (Fig. S4g–i, ESI†). So we chose [hydroxyl of SC4A] : [NaOH] = 1 : 1.2 as the optimized mole ratio for further studies. We found that no film formed when the mass fraction of SC4A was below 2.5%, and when the mass fraction of SC4A was above 7.5%, semitransparent and fragile films formed. Finally, the organic phase was screened among *n*-hexane/acetone/toluene, and *n*-hexane with low toxicity was the best choice. In general, 5% SC4A with 1% NaOH aqueous phase and 0.5% TC in *n*-hexane were the most suitable conditions for fabricating pTC-SC4A films. Similarly, conditions for making pTC-P5A (Table S2 and Fig. S5, ESI†) and pTC-C4A films were also screened progressively, and 2% P5A with 1.6% NaOH and 2% C4A in 0.4% NaOH aqueous phase with 0.5% TC in *n*-hexane were determined to be the optimal conditions.

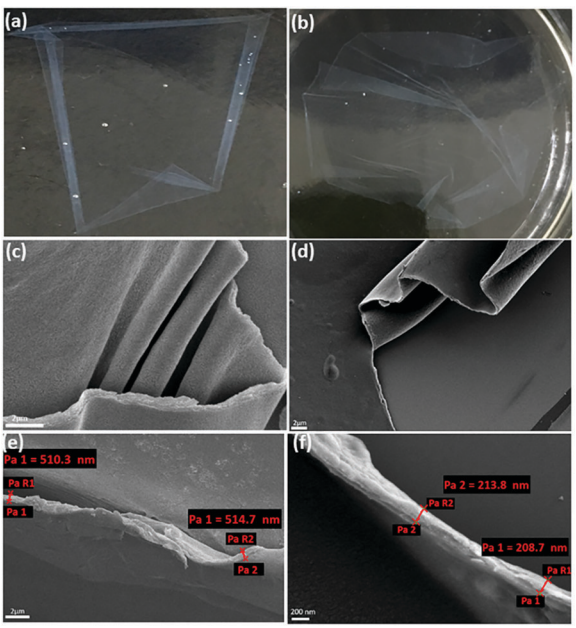

Fig. 3 (a and b) Photos of pTC-SC4A film and pTC-P5A film isolated from the PES support floating in DMF; (c and e) SEM images of the wrinkled edge and cross-section (average thickness: 512 nm) of the pTC-SC4A film prepared *via* PES supported interfacial polymerization under its optimal conditions; (d and f) SEM images of the wrinkled edge and cross-section (average thickness: 211 nm) of the pTC-P5A film prepared *via* PES supported interfacial polymerization under its optimal conditions.

We firstly checked the permeability of the pTC-SC4A, pTC-P5A and pTC-C4A films using various solvents, respectively (as listed in Table 1 and Table S3, ESI†). The thin-films were prepared on nylon6 porous membranes which are insoluble in organic solvents. Fortunately, the permeances of various solvents in the pTC-SC4A film were extremely high, and the solvents could flow across the films at an ultrafast rate even in simple vacuum filtration. The permeance of water in the pTC-SC4A film was up to 1525 L m^{-2} h^{-1} bar^{-1} and the permeance of acetonitrile was even up to 9763 L m^{-2} h^{-1} bar^{-1}. The permeability of the pTC-P5A film was relatively low, and the permeations for organic solvents were faster than water both in pTC-SC4A and pTC-P5A films. These ultrahigh permeances hinted that the thin-films possessed some larger pores rather

Table 1 Permeances (L m^{-2} h^{-1} bar^{-1}) of seven solvents in pTC-SC4A or pTC-P5A films fabricated under their optimal conditions, respectively

Solvents	pTC-SC4A	pTC-P5A
H_2O	1525	610
EtOH	2034	718
DMF	3186	1356
MeOH	4881	1525
Acetone	8136	3051
CH_2Cl_2	6669	2290
CH_3CN	9763	3051

than micro pores. But for the pTC-C4A film, water could not pass through *via* vacuum filtration, which did not match our original design to explore new membrane materials with high transport properties. So, next we only focused on the pTC-SC4A and pTC-P5A films for further characterization.

Comparing the FT-IR spectra of the pTC-SC4A film with SC4A (Fig. S6, ESI†), the peak at 3373 cm^{-1} standing for the intramolecular hydrogen bonding of hydroxyl on SC4A weakened a lot, and the appearance of peaks at 1275 cm^{-1} (C–O) and 1634 cm^{-1} (C═O) suggested the ester formation. Also, the inherited peaks of C–S bonds (1040–1050 cm^{-1}) indicated the existence of SC4A, and the split aromatic C–O (1044 and 999 cm^{-1}) suggested that the hydroxyls in SC4A were incompletely crosslinked.

Similarly, the FT-IR spectrum of the pTC-P5A film (Fig. S7, ESI†) also gave two characteristic peaks of aromatic ester at 1274 cm^{-1} (C–O) and 1635 cm^{-1} (C═O), and the peak at 3239 cm^{-1} referring to P5A's hydroxyl totally disappeared. Scanning electron microscopy (SEM) revealed a crumpled structure of the pTC-SC4A film (Fig. 2c) because the film tended to fold due to low affinity of sulfonate groups with EtOH where the film was stored in. While the quite flat structure over a large area of the pTC-P5A film (Fig. 2d) suggested its EtOH-philic structure. A torn edge was specially picked out and enlarged to see the thin films' structure more clearly (Fig. 3c and Fig. S8 for pTC-SC4A and Fig. 3d and Fig. S9, ESI,† for pTC-P5A). These images showed that smooth films with no defects were successfully fabricated. Further analysis of a cross-section of the film showed that the average thicknesses were 512 nm and 211 nm for pTC-SC4A and pTC-P5A films, respectively (Fig. 3e and f).

Large amounts of both pTC-SC4A and pTC-P5A films were prepared under their optimal conditions to study their inherent physical properties. Thermogravimetric analysis (TGA) showed that both of the films could remain stable up to 150 °C in a nitrogen environment, suggesting their good thermal stability (Fig. S10 and S11, ESI,† blue line). However, the films began to fall apart sharply near 200 °C (Fig. S12 and 13, ESI,† blue line), suggesting the easy degradation of the films after sufficient use. The stability of the films under different pH values was also investigated and both films could remain stable except under strong acidic and alkaline conditions (Fig. S14–S19, ESI†). The surface areas of the pTC-SC4A and pTC-P5A films were measured *via* N_2 adsorption experiments (Fig. S20 and 21, ESI†) and calculated at 123 $m^2\ g^{-1}$ and 85 $m^2\ g^{-1}$ respectively using a multi-point BET method. Density functional theory (DFT) calculations applied to the isotherm curves indicated that the majority size of pores concentrated on 2.7 nm for the pTC-SC4A film (Fig. S22, ESI†) and 3.4 nm for the pTC-P5A film (Fig. S23, ESI†), respectively. These mesopores in the films resulted in higher permeability compared to other micropore films prepared *via* interfacial polymerization.[4,7a,12a,b,15]

As cyclophanes often show selective binding abilities to different kinds of dyes, several dyes were selected for vacuum filtration experiments, which were carried out at room temperature. The concentration of every feed solution was fixed at 1×10^{-5} mol L^{-1} in water and the feed volume was 15 mL per square centimetre for both pTC-SC4A and pTC-P5A films.

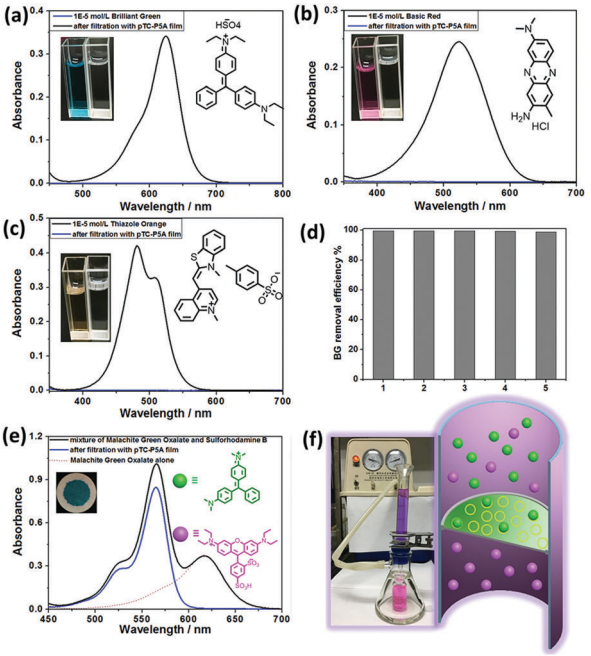

Fig. 4 UV-Vis spectra of dyes before and after filtration with the pTC-P5A film (insert pictures: structures of dyes, photos of solution before and after filtration): (a) BG, (b) BR, (c) TO; (d) consecutive regeneration cycles using BG as a model compound and films were regenerated *via* rinsing with EtOH at room temperature; (e) UV-Vis spectra of MGO and sRhB mixture before (black) and after (blue) filtration with a pTC-P5A film UV-Vis spectrum of sRhB alone is marked as a red dotted line in order to conveniently observe the adsorption effect (insert pictures: structures of MGO (green) and sRhB (pink), photo of the film after filtration); (f) photo (left) and schematic illustration (right) of dye molecules separated by a pTC-P5A membrane.

The removal efficiencies for the dyes were determined using UV-Vis spectroscopy of the filtrates. As shown in Fig. 4a–c, three cationic dyes (brilliant green (BG), basic red (BR) and thiazole orange (TO)) were efficiently removed. Other cationic dyes, such as methylene blue, rhodamine B, ethyl violet, acridine red (AR), malachite green oxalate (MGO), crystal violet, pararosaniline hydrochloride, and 4-[4-(dimethylamino)styryl]-1-methylpyridinium iodide could be all removed both by pTC-SC4A (Fig. S24, ESI†) and pTC-P5A (Fig. S25, ESI†) films, respectively. The video of the removal of AR by the pTC-P5A film showed that AR was only gathered at the top side of the film, suggesting a good performance of the film (Video S2, ESI†).

Owning to the weak binding abilities of the cyclophanes with dyes in organic solvents, the films could be regenerated *via* eluting the dyes with EtOH or acetone at room temperature *via* the same vacuum filtrations. Consecutive regeneration cycles were repeated for five times based on BG as a model compound, which showed >95% removal efficiency (Fig. 4d). Furthermore, these films did not hinder the permeations of negatively charge molecules which often showed small affinities with SC4A and P5A. As shown in Fig. 4e and f, two kinds of dyes (MGO and sulforhodamine B (sRhB)) with opposite charge could be effectively separated by the pTC-P5A film. The anionic sRhB passed through the film very well with the loss less than 5%, and the MGO was totally removed.

In summary, two kinds of mesoporous polymer films based on crosslinked SC4A and P5A have been successfully prepared, which show ultrahigh solvent permeances (up to 9763 L m^{-2} h^{-1} bar^{-1} for acetonitrile in pTC-SC4A based polymer films). The micro-morphologies of the polymers greatly rely on the conditions of the interfacial polymerization. There are two types of pores in the polymer films: one from the polymer network allowing a fast flow rate of solvents, and the other from the cavity of macrocycles trapping small organic dyes. Owing to the ultrahigh permeability and the strong host–guest complexation between the macrocycles and dyes, both of the polymers can effectively remove cationic dyes *via* simple vacuum filtrations. And the absorbed dyes are easily eluted from the polymers by organic solvents and the films could be regenerated to their original states. Furthermore, these polymers could easily separate cationic and anionic dyes as a result of selective molecular recognition. Exploiting macrocycles as building blocks will be a new way to fabricate crosslinked polymers for fast and efficient separations.

This work was supported by the National Natural Sciences Foundation of China (21432004 and 91527301).

Conflicts of interest

The authors have no conflicts of interest to declare for this communication.

Notes and references

1 (*a*) C. A. Martínez-Huitle, M. A. Rodrigo, I. Sirés and O. Scialdone, *Chem. Rev.*, 2015, **115**, 13362; (*b*) M. A. Shannon, P. W. Bohn, M. Elimelech, J. G. Georgiadis, B. J. Mariñas and A. M. Mayes, *Nature*, 2008, **452**, 301; (*c*) D. S. Sholl and R. P. Lively, *Nature*, 2016, **532**, 435; (*d*) R. P. Schwarzenbach, B. I. Escher, K. Fenner, T. B. Hofstetter, C. A. Johnson, U. von Gunten and B. Wehrli, *Science*, 2006, **313**, 1072.

2 (*a*) G. Liu, W. Jin and N. Xu, *Angew. Chem., Int. Ed.*, 2016, **55**, 13384; (*b*) P. Marchetti, M. F. Jimenez Solomon, G. Szekely and A. G. Livingston, *Chem. Rev.*, 2014, **114**, 10735; (*c*) Z. V. Singh, L.-L. Tan, M. G. Cowan, Y.-W. Yang, W. Zhang, D. L. Gin and R. D. Noble, *J. Membr. Sci.*, 2017, **539**, 224; (*d*) X. Li, Z. Li and Y. W. Yang, *Adv. Mater.*, 2018, **30**, 1800177.

3 (*a*) A. Bétard and R. A. Fischer, *Chem. Rev.*, 2012, **112**, 1055; (*b*) P. Falcaro, K. Okada, T. Hara, K. Ikigaki, Y. Tokudome, A. W. Thornton, A. J. Hill, T. Williams, C. Doonan and M. Takahashi., *Nat. Mater.*, 2016, **16**, 342.

4 (*a*) S. Kandambeth, B. P. Biswal, H. D. Chaudhari, K. C. Rout, S. Kunjattu, H. S. Mitra, S. Karak, A. Das, R. Mukherjee, U. K. Kharul and R. Banerjee, *Adv. Mater.*, 2017, **29**, 1603945; (*b*) K. Dey, M. Pal, K. C. Rout, S. Kunjattu, H. A. Das, R. Mukherjee, U. K. Kharul and R. Banerjee, *J. Am. Chem. Soc.*, 2017, **139**, 13083.

5 (*a*) C. M. Lew, R. Cai and Y. Yan, *Acc. Chem. Res.*, 2010, **43**, 210; (*b*) J. Yao and H. Wang, *Chem. Soc. Rev.*, 2014, **43**, 4470; (*c*) M. Y. Jeon, D. Kim, P. Kumar, P. S. Lee, N. Rangnekar, P. Bai, M. Shete, B. Elyassi, H. S. Lee, K. Narasimharao, S. N. Basahel, S. Al-Thabaiti, W. Xu, H. J. Cho, E. O. Fetisov, R. Thyagarajan, R. F. DeJaco, W. Fan, K. A. Mkhoyan, J. I. Siepmann and M. Tsapatsis, *Nature*, 2017, **543**, 690.

6 (*a*) P. Sun, K. Wang and H. Zhu, *Adv. Mater.*, 2016, **28**, 2287; (*b*) G. Liu, W. Jin and N. Xu, *Chem. Soc. Rev.*, 2015, **44**, 5016; (*c*) Q. Yang, Y. Su, C. Chi, C. T. Cherian, K. Huang, V. G. Kravets, F. C. Wang, J. C. Zhang, A. Pratt, A. N. Grigorenko, F. Guinea, A. K. Geim and R. R. Nair, *Nat. Mater.*, 2017, **16**, 1198; (*d*) D.-Y. Koh, B. A. McCool, H. W. Deckman and R. P. Lively, *Science*, 2016, **353**, 804.

7 (*a*) M. F. Jimenez-Solomon, Q. Song, K. E. Jelfs, M. Munoz-Ibanez and A. G. Livingston, *Nat. Mater.*, 2016, **15**, 760; (*b*) S. Kim and Y. M. Lee, *Prog. Polym. Sci.*, 2015, **43**, 1.

8 (*a*) D. Schneider, D. Mehlhorn, P. Zeigermann, J. Karger and R. Valiullin, *Chem. Soc. Rev.*, 2016, **45**, 3439; (*b*) L. L. Tan, H. Li, Y. Tao, X. A. Zhang Sean, B. Wang and Y. W. Yang, *Adv. Mater.*, 2014, **26**, 7027; (*c*) L.-L. Tan, Y. Zhu, H. Long, Y. Jin, W. Zhang and Y.-W. Yang, *Chem. Commun.*, 2017, **53**, 6409.

9 (*a*) Z. Zheng, R. Grünker and X. Feng, *Adv. Mater.*, 2016, **28**, 6529; (*b*) W. J. Koros and C. Zhang, *Nat. Mater.*, 2017, **16**, 289; (*c*) D. L. Gin and R. D. Noble, *Science*, 2011, **332**, 674.

10 (*a*) J. Mulder. *Basic Principles of Membrane Technology*, Springer Science & Business Media, 2012; (*b*) W. Xuan, C. Zhu, Y. Liu and Y. Cui, *Chem. Soc. Rev.*, 2012, **41**, 1677; (*c*) M. Sahimi, *Flow and transport in porous media and fractured rock*, Wiley-VCH, 1995.

11 (*a*) Q. Yang and M. Ulbricht, *Chem. Mater.*, 2012, **24**, 2943; (*b*) J. Meng, J. Cao, R. Xu, Z. Wang and R. Sun, *J. Mater. Chem. A*, 2016, **4**, 11656; (*c*) M. J. Park, G. M. Nisola, E. L. Vivas, L. A. Limjuco, C. P. Lawagon, J. G. Seo, H. Kim, H. K. Shon and W.-J. Chung, *J. Membr. Sci.*, 2016, **510**, 141; (*d*) Q. Zhao and Y. Liu, *Chem. Commun.*, 2018, **54**, 6068–6071.

12 (*a*) M. A. Kamboh, I. B. Solangi, S. T. H. Sherazi and S. Memon, *Desalination*, 2011, **268**, 83; (*b*) E. Akceylan, M. Bahadir and M. Yılmaz, *J. Hazard. Mater.*, 2009, **162**, 960; (*c*) M. Chen, T. Shang, W. Fang and G. Diao, *J. Hazard. Mater.*, 2011, **185**, 914.

13 (*a*) S. J. Barrow, S. Kasera, M. J. Rowland, J. del Barrio and O. A. Scherman, *Chem. Rev.*, 2015, **115**, 12320; (*b*) R. N. Dsouza, U. Pischel and W. M. Nau, *Chem. Rev.*, 2011, **111**, 7941; (*c*) T. Ogoshi, T.-a. Yamagishi and Y. Nakamoto, *Chem. Rev.*, 2016, **116**, 7937; (*d*) M. V. Rekharsky and Y. Inoue, *Chem. Rev.*, 1998, **98**, 1875; (*e*) D.-S. Guo, K. Wang and Y. Liu, *J. Inclusion Phenom. Macrocyclic Chem.*, 2008, **62**, 1; (*f*) Q. Zhao, Y. Chen, S.-H. Li and Y. Liu, *Chem. Commun.*, 2018, **54**, 200–203.

14 (*a*) J. Liu, D. Hua, Y. Zhang, S. Japip and T.-S. Chung, *Adv. Mater.*, 2018, **30**, 1705933; (*b*) L. F. Villalobos, T. Huang and K.-V. Peinemann, *Adv. Mater.*, 2017, **29**, 1606641; (*c*) L. Xiao, Y. Ling, A. Alsbaiee, C. Li, D. E. Helbling and W. R. Dichtel, *J. Am. Chem. Soc.*, 2017, **139**, 7689; (*d*) A. Alsbaiee, B. J. Smith, L. Xiao, Y. Ling, D. E. Helbling and W. R. Dichtel, *Nature*, 2016, **529**, 190; (*e*) N. Morin-Crini and G. Crini, *Prog. Polym. Sci.*, 2013, **38**, 344.

15 S. Karan, Z. Jiang and A. G. Livingston, *Science*, 2015, **348**, 1347.

16 (*a*) S. Fernández-Abad, M. Pessêgo, N. Basílio and L. García-Río, *Chem. – Eur. J.*, 2016, **22**, 6466; (*b*) T. Ogoshi, S. Kanai, S. Fujinami, T.-a. Yamagishi and Y. Nakamoto, *J. Am. Chem. Soc.*, 2008, **130**, 5022.